Microporous and Mesoporous Materials, 2008, 116, 718-722

https://doi.org/10.1016/j.micromeso.2008.06.002

Influence of silanols condensation on surface properties of micelle-templated silicas. A modeling study.

Ettore Fois*, Aldo Gamba, Gloria Tabacchi

Dipartimento di Scienze Chimiche ed Ambientali and INSTM, Universita' dell'Insubria, Via Lucini 3, I-22100 Como (Italy)

Abstract

The dehydration of model mesoporous silicas has been studied via molecular dynamics simulations. By progressively dehydrating the system, initially characterized by an even distribution of surface silanols, patches with hydrophobic or hydrophilic character are formed on the pores surface. It is found that the local concentration of silanols is strictly correlated to the local structure of pores surface, namely hydrophobic and hydrophilic patches are located in high- and low-curvature surface regions respectively, in line with experimental evidences. Simulations suggest that the microscopic origin of both the uneven Si-OH distribution and the pores surface deformation should be related to the dehydroxylation process, which is governed by interactions among the silica matrix.

Key words: molecular dynamics, mesoporous silicas, pores structure, silanols, hydrophilicity

* Corresponding author.
Ettore Fois
DSCA, Universita' dell'Insubria
Via Lucini 3, I-22100 Como (Italy)
e-mail fois@fis.unico.it
FAX + 39 031 326230

Microporous and Mesoporous Materials, 2008, 116, 718-722

1 Introduction

Micelle templated silicas (MTS) [1–4] are a class of mesoporous materials characterized by an ordered lattice of pores in an amorphous SiO_2 matrix. MTS have been the subject of growing interest in the scientific and industrial communities due to their regular distribution of pores, and to the possibility to tune channels size by means of appropriate surfactants. MTS may be exploited in different potential applications, ranging from sorption/separation of bulky molecules [5] to catalysis, [6] sensing [7] and as host structures for novel nanomaterials. [8,9] In this context, a detailed knowledge of the surface structure of MTS would be of primary relevance for the fine-tuning of the properties of these materials as well as for the extension of their field of applicability. However, a thorough understanding of the structure-properties relationships is still lacking due to the amorphous nature of the SiO_2 walls, which makes it very difficult to extract structural information at atomic resolution from experimental data. In this respect, modelling studies via computer simulations may help in providing a microscopic level picture of the surface structure which can be related to observed functional properties. One of these properties is the hydrophilic character of the pores surfaces.
MTS can be described by the general formula $(SiO_2)_m \cdot (H_2O)_n$. The inner surfaces of these materials exhibit different kinds of silicon atoms, labeled Q^{4-n} according to the number n of hydroxyl groups bonded to Si. Surface OH groups are mainly attached to Q^3 silicon atoms, but they may also be present in the form of geminal silanols, i.e. two OH groups bonded to the same Q^2 Si atom. In general, the concentration of silanol groups on the inner surfaces of evacuated MTS determines their degree of hydrophilicity.
Depending on the calcination temperature, MTS with silanol densities ranging from 2 to 5 Si-OH/nm^2 may be obtained. [10] The distribution of Q^{4-n} species can be estimated by magic angle spinning ^{29}Si NMR spectroscopy, [11,12] while information on the hydrogen bond properties of the OH groups may be drawn from ^{1}H solid state NMR experiments [13–15]. NMR studies of MCM-41, both as-prepared and under hydration/dehydration cycles, elucidated the presence of different types of silanols. At high calcination temperature, most of the silanol groups are not involved in hydrogen bonds with other silanols (i.e.: "isolated" silanols), while at lower temperatures hydrogen bonded (i.e.: "vicinal") silanols may be found as well. Moreover, irreversible modifications of the silica surface inside the pores induced by calcination were detected. [10]
IR and adsorption calorimetry data suggested that silanols are not evenly distributed on the channels surfaces; rather, the pores show hydrophobic and hydrophilic regions. [16] The former have a low silanol density and a high concentration of surface siloxane Si-O-Si bridges. In contrast, silanol-rich hydrophilic patches are characterized by a high concentration of Si-OH groups and probe water molecules may be preferentially adsorbed via hydrogen bonds on surface silanols. [16,17] On the basis of EPR/XRD studies, [18] it has been

proposed that hydrophobic patches are mostly localized in high-curvature regions, while flat low-curvature regions host hydrophilic patches.
A detailed knowledge of silanols distribution may be relevant also in MTS post-synthesis treatments. Indeed grafting techniques [19] can be used to functionalize MTS inner surfaces with catalytically active species.[20,21] A reliable microscopic picture of the MTS inner surfaces is of relevance also in ab initio modeling studies.[22]
In the present work, the dehydration process in MTS has been studied by means of classical molecular dynamics (MD) simulations, with the purpose of investigating at a microscopic level the presence and the origin of the uneven silanol distribution in dehydroxylated silicas.
The simulation system was a model mesoporous silica characterized by empty cylindrical pores with an even distribution of Si-OH groups. On such a system, dehydration was modelled by performing successive condensation steps, i.e. by removing H_2O molecules from pairs of vicinal silanols. By monitoring the pores structure and silanol distribution along the simulated dehydration process, correlations could be established between the presence of hydrophobic and hydrophilic patches and local curvature.
An additional factor which might affect the structure/hydrophilicity relationships is the surfactant used in the MTS synthesis. A thorough investigation of the role of templating micelles on MTS structure is out of the scope of this work. Here, in order to single out possible excluded volume effects on the surface properties of these materials, simulations including a coarse-grained model template were performed as well.

2 Methodology

Simulations were performed via the Molecular Dynamics technique using the CP2K computer package. [23] Interatomic potential functions are a crucial ingredient in classical molecular dynamics. Here we have adopted literature central force potential functions. A Born-Mayer type pair potential has been adopted for all the Si-O, Si-Si, and O-O interactions. [24] The augmented CVFF central valence force field has been employed for the H-H, Si-H and O-H interactions. [25] A cutoff distance of 12 Å was applied to the short-range interactions. The Ewald summation technique was adopted for the long-range electrostatic interactions. The initial configuration of the system was built by cutting parallel cylindrical holes of 20 Å diameter in a previously equilibrated amorphous bulk SiO_2. A cubic simulation cell with L=29.43 Å and periodic boundary conditions were adopted. The thickness of the SiO_2 walls was $\sim$ 1 nm. With this arrangement, the infinite cylinders form a square lattice with side equal to the periodically repeated simulation cell. In the cutting process, several unsaturated O and undercoordinated Si atoms were formed on the

pores edges. Dangling bonds on oxygen atoms were saturated with H atoms whereas an equal number of hydroxyls was added to unsaturated Si cations in order to obtain a stoichiometrically hydrated silica. By using this approach a mesoporous SiO_2 model was obtained, where each Si atom was coordinated to four oxygen atoms and each oxygen was coordinated to two atoms (Si or H). With such a procedure, similar to that reported in Ref.[26], the complex polymerization and aggregation process of the silica-micelle mesophase was bypassed.

In the synthesis of real MTS, the pores are evacuated upon calcination, when the template micelles are eliminated. However, in order to study possible template-induced excluded-volume effects on the pores structure in the early stages of the dehydration, we have performed two sets of simulations, one without template model and one where we have modelled a non-deformable cylindrical template. Since an atomistic description of the templating agent is not required for the present purposes, we have adopted a coarse-grained description of the template, which has been modelled by infinite soft cylinders parallel to the z axis. Only Si and O atoms were allowed to interact with the model template via a 24-3 Lennard-Jones type potential:

$$U(r) = 4\epsilon((\sigma/r)^{24} - (\sigma/r)^{3}) \quad (1)$$

The stiff repulsive r^{-24} term was chosen in order to emphasize excluded-volume effects. The r^{-3} attractive part should model the dispersion interactions of a closed-shell species with a continuous surface. [27] Moreover, by keeping into account that neutral surfactants are actually adopted in some MTS syntheses, [28] the total charge of the model templates was set to zero. In this model, interactions between silica matrix and template depend on the radial separation of Si and O atoms from the cylinder axis.

At the best of our knowledge, no example of a mixed atomistic plus coarse grained approach for simulating micelles hosted in silica based materials has been previously reported in literature. In view of this, the parameters of the Si-template and O-template 24-3 potentials had to be determined. Different sets of parameters were tested, on the basis of the assumption that the template should not significantly affect the internal geometry of SiO_4 units. The validity of each set was verified in an a-posteriori fashion by checking that the average short-range structural properties of the SiO_2 matrix in the presence of the template well reproduced those typical of silicates, namely Si-O bond lengths of about 1.61 Å, and tetrahedral O-Si-O angles. The final set of silica-template parameters adopted in production runs is reported in Table 1. Values of σ larger than in Table 1 tend to compress Si-O bonds, while larger ϵ values cause an elongation of such bonds.

Equilibration of the mesoporous silica plus template model (MTS(1)) and of the template-free system (MTS(2)) were performed via several nanosecond-scale simulated annealing runs (i.e. repeated sequencies of fast-heating/slow-

quenching MD simulations). The resulting systems were then simulated at room temperature and their structural properties compared. In all molecular dynamics runs, a time step Δt of 0.5 fs was adopted for the integration of the equations of motion. In each production run, performed in the NVT ensemble at T=300 K, the time evolution of the simulated system has been followed for about 10 ns. Average fluctuations of the conserved quantity (ΔE/E) were monitored along the production runs and were always found lower than 1×10^{-6}. The average fluctuations of the temperature around the target value of 300 K were of the order of 7-8 K, with a maximum amplitude of 22 K.
The starting stoichiometry of both MTS(1) and MTS(2) was $(SiO_2)_{303}\cdot(H_2O)_{57}$, corresponding to an initial silanol density of 6.2 Si-OH/nm^2. These systems were progressively dehydrated up to a final stoichiometry of $(SiO_2)_{303}\cdot(H_2O)_{33}$, corresponding to 3.2 Si-OH/nm^2. Three dehydration cycles were performed for both MTS(1) and MTS(2), leading to silicas characterized by progressively lower Si-OH content ($(SiO_2)_{303}\cdot(H_2O)_{50}$, $(SiO_2)_{303}\cdot(H_2O)_{43}$, $(SiO_2)_{303}\cdot(H_2O)_{33}$). Due to the fact that the pair potential approximation here adopted is not able to reproduce reactive events, the dehydration process was modelled by using a geometrical criterion for removing water molecules.
Each dehydration cycle was composed by three different steps: a) H_2O elimination; b) relaxation; c) thermalization and data collection. The final configuration of a given cycle was used as a starting point for the following one. Let us describe in detail the first dehydration cycle (from $(SiO_2)_{303}\cdot(H_2O)_{57}$ to $(SiO_2)_{303}\cdot(H_2O)_{50}$). The $(SiO_2)_{303}\cdot(H_2O)_{57}$ system was equilibrated for 5 ns and data were collected for 10 ns in the NVT ensemble at 300 K. A list of the vicinal Si-OH pairs was built. Among these pairs, we shortlisted all pairs characterized by OH$\cdots$OH distance shorter than 2.2 Å and H$\cdots$O-H angle in the 105°$\pm$ 20° range. For each of such pairs, one H atom and one OH group were removed from the system (H_2O elimination step). The H and OH removal left a defective surface characterized by three-coordinated Si and unsaturated O atoms. The relaxation step consisted of a 5 ns simulated annealing MD run aimed at the formation of Si-O-Si siloxane bridges. After relaxation, the system was thermalized and data collected for 10 ns in the NVT ensemble at 300 K. Such a procedure was repeated in the two subsequent dehydration cycles. It should be noticed that in all the three elimination steps, all Si-OH pairs fulfilling the above described geometrical criterion were converted into Si-O-Si bridges. However, the relaxation-thermalization processes led to formation of new hydrogen bonded Si-OH pairs. These pairs were subjected to elimination in the subsequent cycle. Only in the third dehydration cycle, which led to the final $(SiO_2)_{303}\cdot(H_2O)_{33}$ system, no hydrogen bonded silanol pairs (fulfilling the elimination criterion) were detected after the relaxation-thermalization process.

Overall, four trajectories for MTS(1) and four for MTS(2) were performed, corresponding to each of the above mentioned different stoichiometries. In each production run, performed at fixed dehydration level, data were collected on

a 10 ns-long trajectory.

Clearly, this procedure suffers from obvious limitations, such as, for instance, the arbitrariness of the chosen geometrical criterion. On the other hand, the manual elimination step is performed on a thermalized configuration sampled along the time evolution of the system and implies the selection of atoms characterized by values of hydrogen bond length and angle corresponding to Si-OH orientations favourable to form a H_2O molecule. Therefore, keeping into account that the present system can only be afforded in the context of a non-first-principles computational framework, the adopted approach should be considered as a reasonable approximation.

3 Results and Discussion

The starting MTS(1) and MTS(2) systems $(SiO_2)_{303}\cdot(H_2O)_{57}$ show an even distribution of silanols on the pores surfaces. Structural properties of MTS(1) and MTS(2) were investigated along the simulated dehydration process by calculating and comparing radial distribution functions ($g(r)$'s). From such an analysis, it emerged that the presence of the model template affects only slightly the MTS structure. Indeed, systems characterized by the same degree of hydration have very close $g(r)$'s both with and without the template. This should reproduce quite reasonably the behaviour in real MTS, because within the polymerized silica matrix, atoms bind through strong covalent bonds, whereas silica-micelle interactions are non-bonding in character. Such a feature was observed throughout the dehydration cycles.
As the MTS(1) and MTS(2) simulations results were very close, only the MTS(2) series will be discussed in detail. The average Si-O bond length was 1.61 Å, the intra-tetrahedral O-O contact was 2.61 Å, while first neighbor Si-Si contact was 3.15 Å. The silanol O-H bonds were 1.02 Å. The average O-Si-O angle was 105°, in line with a tetrahedral SiO_4 structure. In quartz[29], the Si-O distance is 1.609 Å, the O-O average separation is 2.626 Å, and the Si-Si separation is 3.059 Å. The calculated geometrical parameters, which do not significantly change with the degree of hydration, indicate that a reliable representation of the silica matrix has been achieved. Moreover, the concentration of Q^2 and Q^3 Si sites calculated for the final system (1% and 21% respectively) is in line with the corresponding values obtained from solid-state ^{29}Si NMR on calcined MTS samples (below 2% and 20-25% respectively). [10,12]
Let us now describe in detail how the properties of such MTS models evolved during the simulated dehydroxylation process. The $g(r)$'s calculated for the system after the first dehydration step and for the final and most dehydrated system are shown in Figure 1. In both cases, g(r)'s typical of amorphous, partially hydroxylated silicas are found. A small peak at 2.5 Å in the Si-Si $g(r)$ is

present only in the system characterized by the highest dehydration level. It is due to few 2M siloxane rings [30–32] which are formed in the elimination-relaxation process when the Si-OH concentration is low. Formation of strained siloxane bridges due to the silica surface reconstruction in the calcination process was indicated by solid state NMR experiments. [10] As expected, the peak centered at 1.8 Å in the O-H $g(r)$, which is a signature of hydrogen bonding, disappears in passing to the final system. This indicates depletion of the silanol-silanol hydrogen bonds with increasing dehydration. Thus, in the lowest Si-OH content MTS model, silanols are mainly present as isolated Si-OH groups.

Snapshots from the four simulations performed on MTS characterized by different degrees of hydration are shown in Figure 2,a-d. An interesting feature emerges by examining Figure 2: the channel section progressively deforms with decreasing water content, reaching an approximatively elliptical shape at the lowest silanol concentration. By calculating distances between O atoms located on opposite sides of the pores, it was found that the channel section in the dehydrated system could be approximated by equation 2

$$\frac{x^2}{a^2} + \frac{y^2}{b^2} = 1 \tag{2}$$

where the major and minor radius of the ellipse correspond respectively to a=13.1 Å and b=9.3 Å. With such parameters, the average perimeter of the pores section, calculated using equation 3,

$$4 \int_0^{\frac{\pi}{2}} \sqrt{a^2 \sin^2 t + b^2 \cos^2 t}\ dt \tag{3}$$

was 70.98 Å. The corresponding inner surface area was 20.9 nm^2 per simulation cell, and the silanol concentration was 3.2 $SiOH/nm^2$. As evidenced by the $g(r)$'s, only a tiny fraction of surface silanols are hydrogen-bonded to each other in this system, quite in line with NMR and IR data for MTS characterized by similar surface silanol densities. [10,14,16,17,33]
It would be of relevance to examine how the Si-OH groups are distributed on the pores surface. A closer inspection of the MTS surface structure highlights that the pore surface is composed by silanol-rich patches and regions characterized by a lower Si-OH concentration. As shown in Figure 3, the experimentally detected hydrophilic patches should correspond, in our model system, to the flatter sides of the elliptical channels, whereas high-curvature regions are depleted from Si-OH groups and should have therefore an hydrophobic character. By using Equation 2 and 3, the surface area of the hydrophobic and hydrophilic patches was calculated. This allowed us to estimate the Si-OH

density characterizing silanol rich and silanol poor regions, which amounted to 4.0 and 1.8 Si-OH/nm^2 respectively.

4 Conclusions

In the present work, based on an atomistic set of simulations, the dehydration process of a model MTS system was investigated by progressively decreasing the surface silanol density from 6.2 to 3.2 Si-OH/nm^2. The process, corresponding to the evacuation of 1.3 water molecules per nm^2, led to an increase of the pore surface area of 0.1 nm^2 per evacuated molecule. Moreover, water condensation occurred together with a pore section deformation. In spite of the increase of surface area, the elliptical deformation brought about a moderate shrinking of the minimal pore opening, from the inital value of 10 Å, to a value of 9.3 Å.
A correlation can be established between pore deformation and silanols distribution. Silanol-rich hydrophilic patches (4.0 Si-OH/nm^2) are located on the low-curvature surface regions, while hydrophobic silanol-poor regions (1.8 Si-OH/nm^2) correspond to the higher curvature regions.
In conclusion, the present results suggest that major modifications of the MTS surfaces during post-synthesis treatments could be caused by condensation plus desorption of water molecules which leads to surface erosion. While our results are obtained on a simplified MTS model, the reported findings could have general validity. Actually, a correlation between surface curvature and silanol density has been experimentally detected in MCM-41[16–18], which is an MTS characterized by a hexagonal lattice of pores, different from the present model.

References

[1] U. Ciesla, F. Schuth, Micropor. Mesopor. Mater. 27 (1999) 131.

[2] H. Lin, C. Mou, Accounts Chem. Res. 35 (2002) 927.

[3] J. Shi, Z. Hua, L. Zhang, J. Mater. Chem. 14 (2004) 795.

[4] J. S. Beck, J. C. Vartuli, W. J. Roth, M. E. Leonowics, C. T. Kresge, K. D. Schmidt, C. T. W. Chu, D. H. Olson, E. W. Sheppard, S. B. McCullen, J. B. Higgins, J. L. Schenkler, J. Am. Chem. Soc. 114 (1992) 10834.

[5] A. Sayari, S. Hamoudi, Y. Yang, Chem. Mater. 17 (2005) 212.

[6] M. Jia, A. Seifert, M. Berger, H. Giegengak, S. Schulze, W. Thiel, Chem. Mater. 16 (2004) 877.

[7] B. Yuliarto, H. Zhou, T. Yamada, I. Honma, K. Asai, ChemPhysChem 5 (2004) 261.

[8] F. J. Brieler, P. Grundmann, M. Froba, L. Chen, P. J. Klar, W. Heimbrodt, H. A. Krug von Nidda, T. Kurz, A. Loidl, J. Am. Chem. Soc. 126 (2004) 797.

[9] Z. Liang, A. Susha, Chem. Eur. J. 10 (2004) 4910.

[10] J. Trebosh, J. W. Wiench, S. Huh, V. S.-Y. Lin, M. Pruski, J. Am. Chem. Soc. 127 (2005) 3057.

[11] G. Buntkowsky, H. Breizke, A. Adamxzyk, F. Roelofs, T. Emmler, E. Gedat, B. Grünberg, Y. Xu, H.-H. Limbach, I. Shenderovich, A. Vyalikh, G. Findenegg, Phys. Chem. Chem. Phys. 9 (2007) 4843.

[12] I. G. Shenderovich, D. Maurer, D. Akcakayiran, G. Buntkowsky, H.-H. Limbach, G. H. Findenegg, J. Phys. Chem. B 111 (2007) 12088.

[13] B. Grünberg, T. Emmler, E. Gedat, I. Shenderovich, G. H. Findenegg, H.-H. Limbach, G. Buntkowsky, Chem. Eur. J. 10 (2004) 5689.

[14] Y. K. Bae, O. H. Han, Micropor. Mesop. Mater. 106 (2007) 304.

[15] J. Z. Hu, J. H. Kwak, J. E. Herrera, Y. Wang, C. H. F. Peden, Solid State Nucl. Magn. Res. 27 (2005) 200.

[16] A. Cauvel, D. Brunel, F. Di Renzo, E. Garrone, B. Fubini, Langmuir 13 (1997) 2773.

[17] A. Galarneau, F. Di Renzo, F. Fajula, B. Fubini, M. F. Ottaviani, J. Colloid Interface Sci. 201 (1998) 105.

[18] M. F. Ottaviani, A. Galarneau, D. Desplantier-Giscard, F. Di Renzo, F. Fajula, Micropor. Mesopor. Mater. 44-45 (2001) 1.

[19] T. Maschmeyer, F. Rey, G. Sankar, J.M. Thomas, Nature 378 (1995) 159.

[20] L.G.A. de Water, S. Bulcok, A.F. Masters, T. Maschmeyer, Ind. Eng. Che. Res. 46 (2007) 4221.

[21] M. Boutros, Z. Maoui, H. Sfihi, V. Viossat, A. Gedeon, F. Lanay, Micropor. Mesopor. Mater. 108 (2008) 247.

[22] G. Tabacchi, E. Gianotti, E. Fois, G. Martra, L. Marchese, S. Coluccia, A. Gamba, J. Phis. Chem. C 111 (2007) 4946.

[23] *CP2K code* (2008) http://cp2k.berlios.de/

[24] B. VanBest, G. Kramer, R. VanSanten, Phys. Rev. Lett. 64 (1990) 1955.

[25] J. R. Hill, M. C. Freeman, L. Subramanian, *Reviews in Computational Chemistry* Wiley-WHC, New York (2000).

[26] K. Kleestorfer, H. Vinek, A. Jentys, J. Mol. Catal. A 166 (2001) 53.

[27] J. Isrelachvili, *Intermolecular and Surface Forces 2nd Ed.;* Academic Press, New York, 1991.

[28] I. Park, Z. Wang, T. J. Pinnavaia, Chem. Mater. 17 (2005) 383.

[29] L. Levien, C.T. Prewitt, D.J. Weidner, Am. Mineral. 65 (1980) 920.

[30] A. Roder, W. Kob, K. Binder, J. Chem. Phys. 114 (2001) 7602.

[31] E. Fois, A. Gamba, G. Tabacchi, S. Coluccia, G. Martra, J. Phys. Chem. B 107 (2003) 10767.

[32] E. Fois, A. Gamba, G. Tabacchi, S. Coluccia, G. Martra, J. Porous Mat. 14 (2007) 339.

[33] E. Gianotti, V. Dellarocca, M. Marchese, G. Martra, S. Coluccia, T. Maschmeyer, Phys. Chem. Chem. Phys. 4 (2002) 6109.

Figure 1 Radial distribution functions g(r) calculated for the template free models at two different stages of the dehydration process: $(SiO_2)_{303}\cdot(H_2O)_{50}$ (dashed line) and $(SiO_2)_{303}\cdot(H_2O)_{33}$ (solid line).

Figure 2 Snapshots of the template-free model MTS(2) at different hydration degree. Dark gray sticks represent O atoms; Pale gray sticks Si atoms; white sticks represent protons. a) $(SiO_2)_{303}\cdot(H_2O)_{57}$; b) $(SiO_2)_{303}\cdot(H_2O)_{50}$; c) $(SiO_2)_{303}\cdot(H_2O)_{43}$; d) $(SiO_2)_{303}\cdot(H_2O)_{33}$.

Figure 3 Volume filling representation of the template-free $(SiO_2)_{303}\cdot(H_2O)_{33}$ model system. The elliptical shape of the pore section is clearly distinguishable. Gray spheres represent oxygen atoms; white spheres represent H atoms. Si atoms have been omitted for clarity.

	σ (Å)	ϵ (K)
Si-template	9.5252	576.92
O-template	8.4668	576.92

Table 1: Parameters for the 24-3 potential function (U(r)=4ϵ((σ/r)^{24} - (σ/r)^3)) adopted for the template-silica interactions.

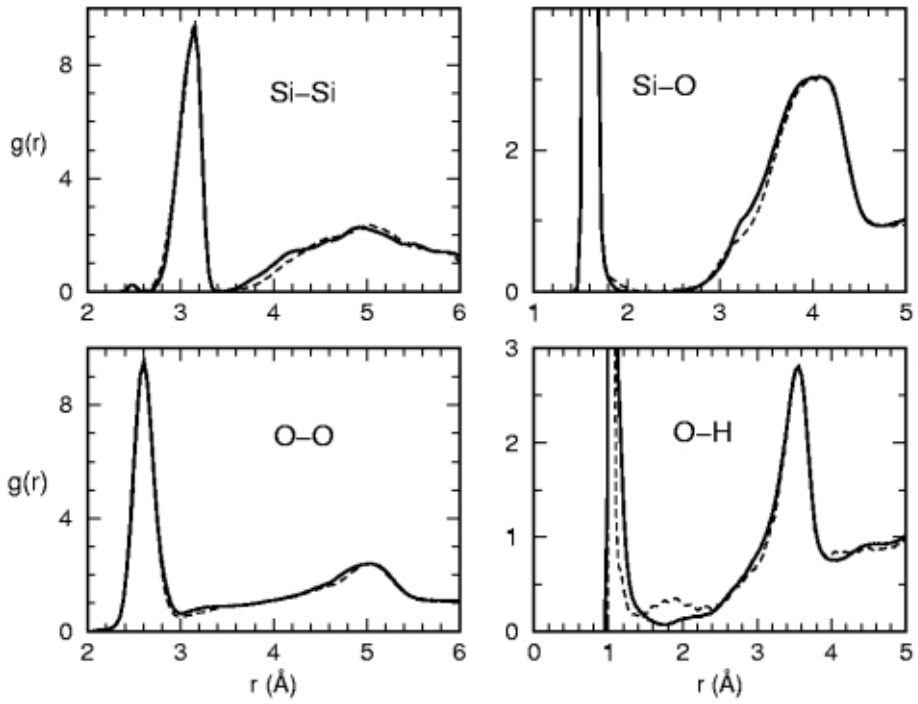

Fig. 1.

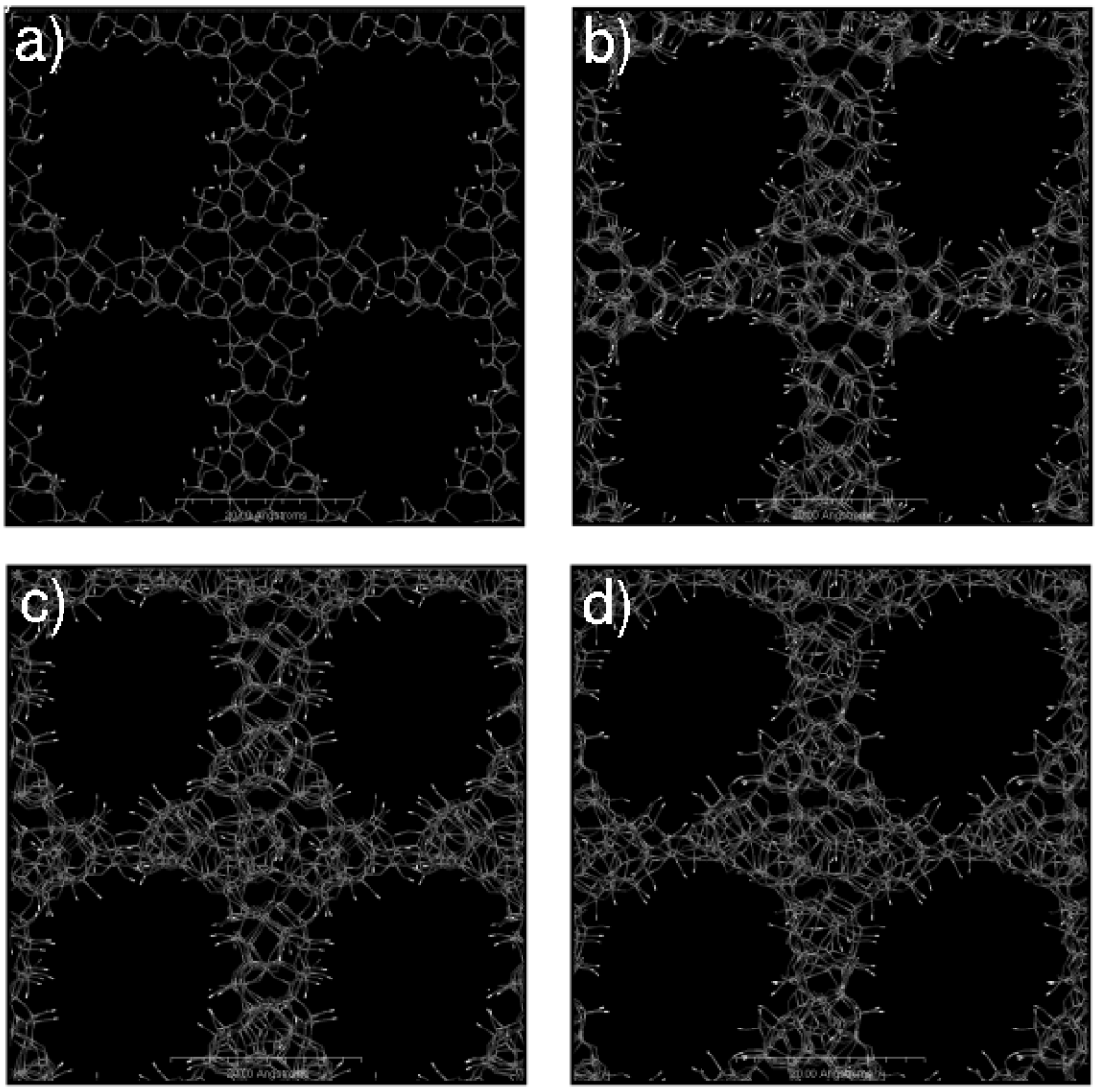

Fig. 2.

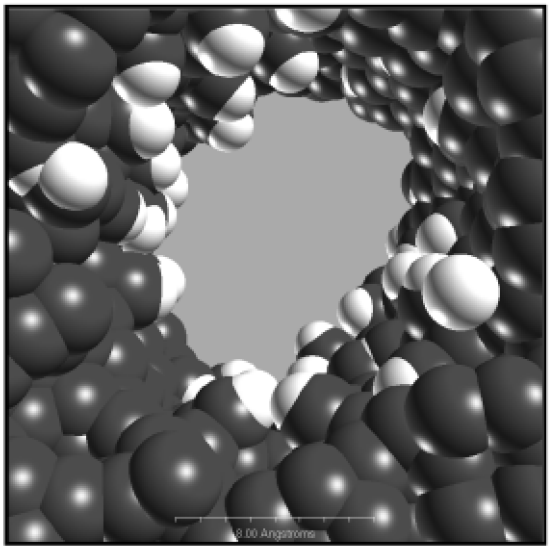

Fig. 3.